AD651225

THE DISSOCIATION RATE OF HYDROGEN FLUORIDE

BEHIND INCIDENT SHOCK WAVES

DR. JAY A. BLAUER

TECHNICAL REPORT AFRPL-TR-67-66

MARCH 1967

AIR FORCE ROCKET PROPULSION LABORATORY
RESEARCH AND TECHNOLOGY DIVISION
AIR FORCE SYSTEMS COMMAND
UNITED STATES AIR FORCE
EDWARDS, CALIFORNIA

52

THE DISSOCIATION RATE OF HYDROGEN FLUORIDE

BEHIND INCIDENT SHOCK WAVES

Dr. Jay A. Blauer
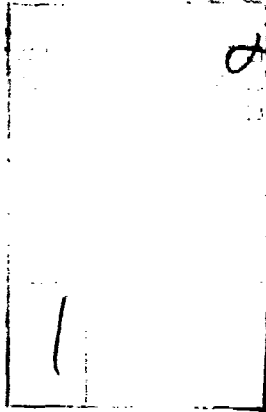
TECHNICAL REPORT AFRPL-TR-67-66

March 1967

Distribution of this document is unlimited.

AIR FORCE ROCKET PROPULSION LABORATORY
RESEARCH AND TECHNOLOGY DIVISION
AIR FORCE SYSTEMS COMMAND
UNITED STATES AIR FORCE
EDWARDS, CALIFORNIA

NOTICES

FOREWORD

This report contains the results obtained during one phase of the Air Force Rocket Propulsion Laboratory Project 314801101, Shock Tube Kinetic Studies. The period covered is from January 1965 to December 1966.

This study was conducted by the author at the Air Force Rocket Propulsion Laboratory. The author wishes to acknowledge his appreciation to Dr. T. E. Jacobs and Dr. N. Cohen of Aerospace Corporation, El Segundo, California, for lending assistance in the planning and data-reduction phases of the research described herein. All calculations necessary to this study were conducted by Aerospace Corporation.

This report has been reviewed and approved.

ELWOOD M. DOUTHETT
Colonel, USAF
Commander

ABSTRACT

The rate of dissociation of hydrogen fluoride behind incident shock waves has been studied in the temperature range of 3700 to 6100° K. Gaseous mixtures containing 0 to 4% hydrogen fluoride, 0 to 6% molecular fluorine, and 0 to 0.5% molecular hydrogen in an argon carrier were used in this study. The course of the dissociation was followed by monitoring the emission intensity of the 1-0 band of hydrogen fluoride at $2.5\,\mu$.

Resort was made to a determination of initial reaction rates to obtain values for the rate constant of the reaction $HF + M = H + F + M$. The expression $k_1 = \dfrac{0.47 \times 10^{19}}{T}\, e^{-134100/RT}$ was found to give the best fit to all of the data. The effect of excess fluorine upon the initial reaction rate demonstrated that the reaction $F + HF = F_2 + H$ is inconsequential to the present study. Similarly, it was found that atomic fluorine has roughly the same third-body efficiency as argon for the recombination of H and F.

Computer calculations based upon the whole reaction profile and including all the data indicate a value for the rate of the hydrogen exchange reaction, namely, $HF + H = H_2 + F$, of $k_2 = 2 \times 10^{12} e^{-35000/RT}$

The data were too scattered to allow an accurate determination of the temperature dependencies of the pre-exponential factors.

ii

TABLE OF CONTENTS

THE DISSOCIATION RATE OF HYDROGEN FLUORIDE

BEHIND INCIDENT SHOCK WAVES

I. INTRODUCTION

With the increasing use of energetic but unfamiliar or less understood chemicals in propellant formulations, kinetic considerations become of increasing importance. When working knowledge of these substances is lacking, kinetic data must supplement other data to allow optimum design and utilization of new propellant systems.

A shock tube is one tool which can be used to generate the conditions of temperature and pressure of interest without a previous time-temperature history of the reacting gas. A rapid response measuring technique, such as the infrared emission method described herein, can then be used to follow the course of the reaction as a function of time.

When this program was initiated, no published data were available concerning the dissociation of hydrogen fluoride, although two other studies[1,2] of the subject were under way at other laboratories.

II. DISCUSSION

A. BACKGROUND

1. Calculation of Shock-Wave Parameters

The Rankine-Hugoniot equations were used in the calculation of the state of the gas immediately behind the shock wave. When fluorine was added to the mix, it was found necessary to assume it to be completely dissociated within the shock wave at all temperatures considered. This was necessary because of the extreme instability of molecular fluorine[3] under the experimental conditions.

1

The shock velocities necessary to define the conditions of the reacting gas were obtained by means of spark-gap shock detectors accurately spaced at known distances along the tube. The spark plug signals were displayed on an oscilloscope equipped with a rastor sweep. Superimposed upon this trace was a signal from a crystal-driven timing generator. Hence, the timing trace enabled an accurate determination of shock-wave velocity. The data were fitted to a quadratic equation of the form

$$t = AX + BX^2 \tag{1}$$

Where A and B are constants, t is the elapsed time, and X is the distance traveled by the shock wave. The parameter B is then a measure of the attenuation suffered by the shock wave as it traveled down the tube (about 1%).

The shock velocity at the test station was evaluated from the test data by means of the equation

$$V = \frac{1}{A + 2BX} \tag{2}$$

with a standard deviation of

$$S_V = (S_A + 2XS_B)V^2 \tag{3}$$

Where S_V, S_A, and S_B are the standard deviations of V, A, and B respectively. The value of S_V was usually about 1 to 1.5% of the value of V.

2. Reduction of Rate Data

In this study, the course of the reaction was followed by monitoring the emission intensity of the 2.5-micron band of hydrogen fluoride as a function of time. Consequently, it becomes necessary to relate the measured intensity to the density of unreacted HF in the test gas.

2

The emission intensity was converted to voltage by means of an infrared detector. The voltage was displayed as a function of time on an oscilloscope.

The emission intensity will be given at any time by the following relationship:

$$R = \int_{\Delta\omega} R^o_\omega(T)\epsilon\omega(T)g(|\omega-\omega_o|)d\omega \tag{4}$$

where $R^o_\omega(T)$ and $\epsilon\omega(T)$ are the Planck blackbody function and the spectral emissivity of HF respectively at temperature T. The quantity of g $(|\omega-\omega_o|)$ is the slit function for the spectrometer and is a measure of detection efficiency of the apparatus for radiation of frequency ω when it is set to detect radiation of frequency ω_o. The slit function for our spectrometer is triangular with a half-width of 560 cm^{-1} when it is centered at 4000 cm^{-1}.

The Doppler half-width for rotational lines is given by the expression[4]

$$b_D = (\frac{2kT\ell n_2}{mc^2})^{1/2}\omega_o \tag{5}$$

where c is the velocity of light, m is the mass of the rotating body, and ω_o is the frequency, in wave numbers of the radiation. At 5000°K equation (5) gives a Doppler half-width of 0.023 cm^{-1} for the rotational lines of HF centered in the 2.5-micron band. A collision half-width for broadening of the rotational lines of HF by Ar at 293°K may be estimated at 0.03 cm^{-1} based on the data of Oksengorn[5]. The theoretical temperature dependence of $T^{-1/2}$ for collision broadening then gives a value of 0.007 cm^{-1} for the collision half-width at 5000°K[4]. A comparison of these half-widths indicates that one can select the experimental conditions based upon

3

calculations which employ the Doppler shape for the rotational lines without incurring significant error.

Detailed theoretical calculations of the spectral emissivities of HF were reported by Malkmus [6] who based his results upon Kniper's [7] experimentally determined value of 314 $cm^{-2}atm^{-1}$ at 117°C for the integrated intensity of the fundamental. These calculations were made for four different optical densities ranging from 10^{-2} to 10 atm-cm at each of four temperatures ranging from 1800°K to 7000°K.

Based on the spectral emissivities given by Malkmus, it is possible to evaluate the integral appearing in equation (4) as a function of both optical density and temperature. The required values for the slit function of our apparatus are given by

$$g\left(|\omega-\omega_o|\right) = 1 - \frac{1}{560}\left|\omega-\omega_o\right| \text{ for } |\omega-\omega_o| \leq 560$$
$$= 0 \qquad\qquad \text{ for } |\omega-\omega_o| \leq 560 \qquad (7)$$

Values for the Planck blackbody function were calculated from the following relation:

$$R_\omega^o(T) = \frac{2\Pi hc^2\omega^3}{e^{hc\omega/kT}-1} \qquad (8)$$

Figures 1 and 2 illustrate this spectral radiancy integral, equation (4), as functions of optical density and temperature respectively. A close inspection of these two figures reveals that if the optical density does not exceed $10^{-0.5}$ atm-cm, the radiancy, R, will not only be a nearly linear function of optical density, but will also be independent of temperature provided the temperature does not fall below 3500°K. Accordingly, these limits define the optimum experimental conditions and are met by our equipment behind incident shocks for 2.5% HF in Ar at an initial total

4

pressure of 40 mm Hg. If the experimental conditions are held within these limits, one can write

$$\frac{R}{R_o} = \frac{\rho_T}{\rho_{T_o}} \tag{9}$$

with an error of not more than 10%. Here ρ_T refers to the density of HF behind the shock and the subscript zero refers to the initial conditions.

The proposed kinetic scheme is given by the following series of equations:

$$HF + M = H + F + M \tag{10}$$

$$HF + H = H_2 + F \tag{11}$$

$$H_2 + M = 2H + M \tag{12}$$
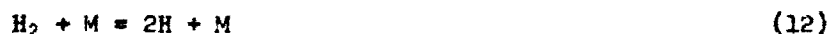
The fluorine exchange reaction and the subsequent fluorine dissociation reaction

$$HF + F = H + F_2 \tag{13}$$

$$F_2 + M = 2F + M \tag{14}$$

are not favored due to the high endothermicity of reaction (13) in reference to reaction (11).

If f is the fraction of HF dissociated at time t and C is the original weight fraction of HF in the gaseous mixture, the density of HF in the gaseous mixture behind the shock wave at time t will be

$$\rho_T = (1-f)C\rho g \tag{15}$$

where ρg is the total gas density behind the shock wave. Differentiation of equation (15) with respect to time yields(for the region immediately behind the shock wave, i.e., for the initial conditions

5

of dissociation of HF)

$$\dot{\rho}_T = C\dot{\rho}_g - \dot{f}C\rho_g \qquad (16)$$

Equations (9), (15), and (16) can now be combined to give for the initial conditions of reaction

$$\dot{f} = \frac{\partial \ln \rho_g}{\partial t} - \frac{\partial \ln R}{\partial t} \qquad (17)$$

It can readily be shown on the basis of the equations of conservation that

$$\frac{\partial \ln \rho g}{\partial t} = \frac{\dot{f}CR}{M_{HF}} \left\{ \frac{A \cdot T - D \cdot D_{HF} \left[1 + \left(\frac{CH_2}{C}\right) \left(\frac{MHF}{MH_2}\right) \left(\frac{D_{H_2}}{D_{HF}}\right) \left(\frac{\dot{f}_{H_2}}{\dot{f}}\right) \right]}{A(u - DRT) - (DR) T} \right\} \qquad (18)$$

Where the symbols not already defined have the following definitions:

R = the gas constant.

M_{HF} = the molecular weight of HF.

$$A = \left[\frac{C_{AR}}{M_{AR}} + \frac{C_F}{M_F} \cdot \frac{3}{2} R + \frac{C_{H_2}}{M_{H_2}} \cdot \overline{C_{vH_2}} + \frac{C}{M_{HF}} \cdot \overline{C_{vHF}} \right]$$

C_{AR} = the weight fraction of argon in the initial shocked mix.

M_{AR} = the molecular weight of argon.

C_F = the weight fraction of atomic fluorine in the initial shocked mix.

M_F = the atomic weight of atomic fluorine.

C_{H_2} = the weight fraction of hydrogen in the initial shocked gas.

M_{H_2} = the molecular weight of hydrogen.

$\overline{C_{vH_2}}$ = the specific heat of hydrogen at constant volume, averaged over the temperature step across the shock wave.

$\overline{C_{vHF}}$ = the specific heat of hydrogen fluoride at constant

6

volume averaged over the temperature step across the shock wave.

D_{HF} = the dissociation energy of gaseous hydrogen fluoride.

D_{H_2} = the dissociation energy of hydrogen.

$\dot{f}_{H_2}$ = the rate of dissociation of hydrogen.

u = the gas velocity relative to the shock wave.

$$D = \frac{C_A}{M_A} + \frac{C_F}{M_F} + \frac{C_{H_2}(1 + \dot{f}_{H_2})}{M_{H_2}} + \frac{C_{HF}(1 + \dot{f})}{M_{HF}}$$

Equations (17) and (18) may now be solved for $\dot{f}$, the result being

$$\dot{f} = \left\{ \frac{CR}{M_{HF}} \left| \frac{A \cdot T - D \cdot D_{HF}}{A(u^2 - DRT)-(DR)^2 T} \right| -1 \right\}^{-1} \left\{ \frac{\dot{f}_{H_2} \cdot C_{H_2} \cdot R}{M_{H_2}} \right.$$

$$\left. \left| \frac{1}{A(u^2 - DRT)-(DR)^2 T} \right| + \frac{\partial \ell nR}{\partial t_\ell} \cdot \frac{1}{\rho_{21}} \right\} \quad (19)$$

Where ρ_{21} is the total gas density ratio across the shock waves. The factor of $1/\rho_{21}$ accounts for the time compression effect converting the laboratory time t_ℓ to particle residence time.

Equation (19) offers a ready means of obtaining an estimate of k_1, the forward rate of reaction (10), since by definition

$$\dot{f} = k_1(M)_o (HF)_o - k_{-1}(M)_o(H)_o(F)_o + k_2(H)_o(HF)_o - k_{-2}$$

$$(F)_o(H_2)_o \quad (20)$$

Where k_2 and k_{-2} refer to reaction (11). For the initial condition of dissociation

$$(H)_o = 0$$

$$(F)_o = 0$$

7

and for mixes containing initial atomic fluorine

$$(H_2)_o = 0$$

$$(H)_o = 0$$

It follows that if the density of HF can be monitored during the very early stages of the reaction, the value of k_1 can be obtained from the initial slope of the reaction profile as recorded on the oscilloscope.

The overall reduction of the rate data proceeds by matching observed and calculated reaction profiles. This necessitated having a set of initial estimates of the rates of equations (10) through (12). The initial estimate of k_1 was obtained by taking the initial slopes of the observed reaction profiles as described above. The initial estimate of k_2 was taken from reference 1, the value being

$$k_2 = 1 \times 10^{13} e^{-35000/RT} \tag{21}$$

The value of k_{-3} the reverse rate of reaction (12), was also taken from reference 1, the value being

$$k_{-3} = 10^{18.3} T^{-1} \tag{22}$$

Since the density of excess hydrogen was not widely varied, no attempt to improve k_{-3} was made. The reverse rates of all three reactions were computed from the forward rates and thermodynamic data.[8] The reaction profile was then computed from the estimates of all the rates coupled with the shock parameters. The profiles were calculated by an integration technique with time and temperature as interdependent variables. Computer analysis was necessary since the reaction temperature changes by as much

8

as 1000°C during the course of the reaction (see Table II). Several oscilloscope traces representing typical reaction profiles are illustrated in Figure 7.

In comparing observed and calculated reaction profiles, it becomes necessary to know the initial height of the observed profile. This necessitated a usable extrapolation procedure. A simple logarithmic expression of the form

$$\log E = \log E_o^o - \frac{t_\ell}{\tau} \qquad (23)$$

was found to fit the data for the early stages of reaction in nearly every instance. In this expression, τ and E_o^o are constants, the value of E_o^o being the initial height of the voltage trace (see Figure 8). Accordingly, initial intensities were obtained by simple logarithmic extrapolation.

In the computer analysis, M in equations (10) and (11) was considered to be any third body. After comparing observed and computed profiles, new estimates of the rates were made and the process repeated. Only the pre-exponential factors of the rates were changed in this process, it being assumed that the activation energies for reactions (10) and (11) are approximated by their respective endothermicities.

B. EXPERIMENTAL

1. Shock Tube

The shock tube is of stainless steel and has an inside diameter of 1.5 inches. The overall length of the test section is 25 feet, and the entire inside surface is finished to a grade 8 smoothness.

9

The driver has an overall length of 66 inches. The driver section was static-tested to 20,000 psi and the downwind section to 4000 psi. The driver pressurizing manifold was connected to 10,000 psi helium and 6000 psi nitrogen supply lines. The downwind section emptied into a 55-gallon dump tank. The driver and downwind sections were separated by means of a scribed steel diaphragm designed to burst at a preselected pressure. The downwind section and the dump tank were separated by means of a thin sheet of mylar.

2. Shock Velocity Recording System

Automobile spark plugs of type 45XL whose points were filed smooth were fitted flush with the inside wall of the downwind section of the shock tube at intervals of 30 inches ($\pm$ 0.015 inches). The spatial resolution of these plugs was approximately 1 mm. Spark plugs were also placed 5 1/4 inches from each side of the observation port. A circuit diagram of the associated electronics is shown in Figure 3. The electronic system was designed by Avco Research Company of Wilmington, Massachusetts. One spark signal box was provided for each spark plug. The outputs, from J1, of all boxes were fed to a Tektronix 535 oscilloscope equipped with a rastor sweep. Timing markers were placed at 50μsec. intervals along the sweep by means of a Radionic Model TWM-2A crystal-driven timing generator. The oscilloscope trace was recorded on a 3000-speed polaroid film by means of a Fairchild Model 296 camera. Data were taken directly from the film with the aid of a ruler graduated in units of 1/50th of an inch. The data could be read in this manner

10

with a reproducibility of 0.5%.

3. Observation Port

Synthetic sapphire was selected as the best compromise window material. Sapphire transmission lies between 80-90% from the visible to 5.5μ. The good mechanical strength of sapphire permits tube pressures of 5000 psi.

The two transmission windows are held in compression by close-tolerance brass collets. The collets are retained in the section by hollow nuts. Window-to-shock-tube sealing is effected with indium wire gaskets.

4. Infrared Spectrometer

The analytical system* (Figure 4) consists of two sub-systems: (a) a source system from which blackbody light can be collected and imaged in the shock tube for absorption measurements, and (b) the radiometric system in which light from or through the shock tube is spectrally re-solved by a Perkin-Elmer prism monochrometer.

The system is designed to employ a dual-element detector, which, in conjunction with an adjustable light mask, permits simultaneous two-path measurements. Detector output is amplified and displayed on an oscilloscope.

Absorption measurements may be taken with or without optical chopping. A removable chopper, consisting of an air turbine directly driving a 90-slot wheel, may be positioned at a focal plane on either

---

11

sub-system.

The detector used in this study is of the indium antimonide
variety used in a photoconductive mode. The two detector elements are
separately biased by a 16.2-volt mercury battery shunted with a 100-
kilohm potentiometer, as shown in Figure 5. Bias current is measured
while the detector is operative and adjusted for optimum signal-to-
noise ratio. The entire optical signal is focussed on one detector
element. The outputs of both elements are then fed to a Tektronix 555
dual-trace oscilloscope where the difference in the two signals is dis-
played and photographed.

The signal amplifier consists of two stages of capacitance-
coupled cascode amplification with cathode followers for interstage
coupling and as output stages (see Figure 6). A feedback loop from the
cathode of the output stage to the cathode of the input stage is used
to obtain an overall amplifier gain of about one thousand. Two of these
amplifiers are used, each with its own filament supply and power supply
decoupling filter.

Wire screens of known blocking efficiency for radiant energy
were placed between the detector and blackbody source to test the
linearity of the response of the detector to radiant intensity. The
linearity was found to be good to within 5% over the whole range of
detector response. The signal-to-noise ratio obtainable with the system
varied from 30 to 1 to as high as 150 to 1, depending upon the amplifica-
tion required for the particular shot.

A lower limit for the time resolution of the detector can

be estimated from the shapes of reaction profiles taken at temperatures below the point of observable reaction (see Figure 7a). The equation

$$\frac{dE}{dt} = \frac{1}{\tau} (E_o - E) \tag{24}$$

describes these data with good precision and gives a value of 3.5μ sec. for τ at 3231°K corresponding to Figure 7a. At higher temperatures, the time resolution will improve due to the shorter time required for the shock wave to pass through the width (approximately 1 mm) of the gas envelope in which the HF content is monitored. The upper limit of time resolution is approximated by the rated time constant of the detector itself which is given by the manufacturer[*] as 2μ sec.

A Beckman DU was used as the source of 4000 cm^{-1} light to measure the slit function of the instrument. The resulting slit function was found to be triangular with a half-width of 560 cm^{-1} when the slit of the Perkin-Elmer monochromecer was open to 2 mm.

5. Data Read-Out from Spectrometer

The emission intensities were recorded as a function of time on 3000-speed Polaroid film by photographing the single sweep of the Tektronix 555 dual-beam scope to which the detector outputs were fed. Prior to each shot, accurate voltage marks were placed on the film by means of an SRC[**] Model 3512B DC power supply, calibrated to

---

[*] Santa Barbara Research Center, Goleta, California.

[**] Systems Research Corporation

13

1.0 mv accuracy at three-month intervals. Timing marks were placed on the film by means of a Radionix Model TWM crystal-driven timing generator.

Transparencies were made of the photographic records and these were enlarged and superimposed on 10 x 10 to the centimeter standard graph paper by means of a projection lantern.

6. Gauges

Heise gauges were used for all sample preparations. These gauges were equipped with stainless-steel Bourdon tubes. These proved very reliable in the presence of fluorine gas. The lack of change in the 90-day calibration was very good, the largest error in their use being in reading the dial. This reading error was about 0.1% of the maximum gauge pressure.

A Wallace & Tiernan Model FA-15 gauge was used to measure gaseous pressure in the shock tube itself prior to each shot.

Thermocouple gauges purchased from Veeco* were used to detect the evacuation point (approximately 1μ) of the shock tube prior to charging it with test gas for each shot.

7. Gaseous Purities

a. Hydrogen Fluoride

Hydrogen fluoride having a minimum stated purity of 99.9% was purchased from Matheson and used without further purification. A mass spectrum of the gas as received with argon as an internal

---

*Vacuum Electronics & Equipment Corporation.

14

standard indicated the presence of approximately 0.1% O_2, 0.03% N_2, and trace amounts of SiF_4 as the only detectable impurities.

b. Argon and Hydrogen

Argon and hydrogen having minimum purities of 99.998% were purchased from Matheson and used without further purification. A mass spectrometric analysis indicated only trace amounts of H_2O and N_2 in each gas, i.e., less than 0.01% impurities.

c. Fluorine

Gaseous fluorine with a minimum stated purity of 98.2% was purchased from Allied Chemical Company. A mass spectrometric analysis revealed the presence of about 0.7% O_2 and 0.2% HF. Before use, the gas was passed over NaF pellets for removal of all HF. The resulting gas was used without further purification.

8. Cleaning and Passivation Procedures

Prior to any gas mixing operations the entire system, including the shock tube itself, was flushed with liquid freon, after which everything was purged with nitrogen until dry. After evacuating the system overnight, gaseous fluorine at 50 psi was admitted and allowed to stand for two hours, after which the apparatus was again flushed with nitrogen, the gases being passed into a propane burner which was vented to the outside of the building.

After the system had been passivated, it was kept evacuated at all times except when in use.

9. Sample Preparation and Analysis

Mixtures of Ar and F_2 containing from 0.1 to 10.0% F_2 were prepared and stored in stainless steel mix tanks. The partial pressure of

15

F_2 in each mix was determined during the mixing operation by noting the pressure increase in the vessel as each gas was added. The optical density of each sample was then determined at 285 mμ by means of a Beckman DK-2 recording spectrophotometer. The absorption cell was of stainless steel, had a pathlength of 7.5 cm, and was equipped with 1/8" thick sapphire windows. An inlet and an outlet were placed at opposite ends of the cell to allow flushing it with sample prior to each reading. All optical densities were read at a total pressure of 50 psi. Repeated readings of optical densities over a period of four weeks revealed no change. The extinction coefficients for F_2 determined from these measurements were used in all subsequent gas analyses. Beer's law was found to describe the data over the entire range.

In a manner similar to that described above, samples of HF and Ar were prepared and stored. After sitting overnight, the optical absorption cell was flushed with sample until no changes in the optical densities of the sample at 2.5μ and 2.41μ were observed with additional flushing. After recording the final value of the optical density, the gaseous mixture was passed into distilled water and the argon was collected by displacement. The resulting acidic solution was titrated with standard NaOH with phenolphthalein as indicator. In this manner, the actual partial pressure of HF in each mix was determined simultaneously with its optical density. The extinction coefficients for HF determined in this manner were reproducible to within 5%. All optical densities were again determined at a total pressure of 50 psi. In agreement with the results

16

of Spinnler[2], the results were well-defined by Beer's law up to a total HF pressure of 2.0 psi. This limit was observed in all subsequent measurements.

Individual mixes of argon with each reagent gas were prepared in the ratio of 10:1 and stored in stainless steel mix tanks. The partial pressure of each reagent gas in its respective mix with argon was determined during the mixing operation with the aid of a Heise gauge having a usable range of 0 to 500 psi. The mixes were each prepared at a total pressure of 200 psi.

Gaseous samples for dissociation studies were prepared by mixing pre-selected amounts of each the diluted reagent gases with argon and storing in stainless steel mix tanks.

The partial pressure of H_2 in mixes containing added hydrogen was determined by pressure difference during the mixing operation. The accuracy of this determination was approximately 2% over all. These samples were used within 48 hours of preparation to avoid any concentration changes which might occur on standing.

The partial pressures of HF and F_2 in the gaseous mixtures were determined immediately before use from optical density measurements in the appropriate spectral ranges, always at a total pressure of 50 psi.

10. Data Run Procedure

a. Before each shot, the shock tube, optical absorption cell, and all interconnecting lines were evacuated to 1×10^{-3} torr. The leak rate was found to be of the order of 2×10^{-3} torr/min.

b. The time and calibrated voltage markers were placed on the

17

film in preparation for the planned shot. Trigger circuits and spark plug voltages were adjusted to the proper levels.

c. The indium antimonide detector was cooled with liquid nitrogen and all of its associated electronics were activated. Alignment of the detector was accomplished with the aid of the optical chopper and blackbody source. After alignment was accomplished, the blackbody source was extinguished.

d. The test gas was now introduced into the shock tube and allowed to remain there for 10 to 15 minutes at a total pressure greater than that of the initial pressure of the planned shot. The optical absorption cell was flushed with sample gas during this period until no further change in optical density at 2.5μ was observed with continued flushing. The shock tube was again evacuated to 1×10^{-3} torr, after which it was refilled to the desired pressure with test gas. This preliminary conditioning of the shock tube was necessary to allow saturation of the walls with adsorbed HF. Only after these precautions were taken could reproducible results be obtained. The gaseous pressure in the shock tube was determined with the aid of a Wallace and Tiernan gauge having a usable range of 0 to 200 mm. The pressure could be read accurately to the nearest 0.2 mm.

e. The driver section was immediately pressurized with helium until the diaphragm burst, initiating the shock wave. The elapsed time between the tube-filling operation and the initiation of the shock wave never exceeded 2 minutes.

f. The contents of the dump tank and shock tube were passed

into the propane burner. The entire system was then purged for 15 minutes with low pressure N_2 (ca. 200 psi), after which the metal and mylar diaphragms were replaced and the shock tube reevacuated.

11. Background Emission Intensity

Several shocks were initiated in mixtures of the reagent gases which contained no HF. The resultant oscillograms showed no detectable radiation at 2.5μ to $7000^\circ K$. Accordingly, no background intensity was assumed in the analysis of the data.

III. RESULTS AND INTERPRETATION

A. Internal Consistency of Initial Emission Intensities

Several shocks were initiated in test gases under identical conditions of detector bias current and amplifier plate voltage. The results should lend themselves well to a test of the validity of the assumptions made in the derivation of equation (9).

In Table I the observed initial emission intensities for several shocks are listed as functions of both the initial concentration of HF in the mix and the temperature of the gas. The ratios of initial emission intensity to the initial concentration of HF are shown in column 5 of the table. It is seen that concentration varies by a factor of 5 and the temperature by $3000^\circ C$. Although there is 30% scatter in the data, it is immediately apparent that within experimental error equation (9) is valid.

B. Rate Constants from Initial Rates

Equations (19) and (20) were used to compute initial estimates for the forward rate of reaction (10). The initial slopes of the observed reaction profiles were estimated with the aid of equation (23). The

19

resultant estimates of k_1 are shown in Figure 9 as a function of the reciprocal absolute temperature. The results are also tabulated in Table II.

An analysis of the results illustrated in Figure 9 shows that large amounts of initial, monatomic fluorine in the reacting mix have no significant effect upon the initial reaction rate. If reaction (13) made a significant contribution to the rate of disappearance of HF, the initial rate of reaction would be given by

$$\dot{r} = k_1(M) + k_4(F) \qquad (25)$$

where k_4 is the forward rate of reaction[13]. Under these circumstances an increase in the initial rate would be observed due to the contribution of the second term on the right. The absence of this effect (see Figure 9) can only mean that the contribution of reaction (13) to the rate of disappearance of HF is insignificant compared with the contribution of reaction (10).

Also shown in Figure 9 are Arrhenius-type models fitted to the data with T^{-1} and T^{-2} temperature dependencies for the pre-exponential factor. As can be clearly seen from the figure, the data are not of sufficient accuracy to distinguish between the two forms. The resulting expression for k_1

$$k_1 = \frac{0.47 \times 10^{19}}{T} e^{-134100/RT} \qquad (26)$$

compares favorably with the value obtained by Jacobs et al[1], i.e.,

$$k_1 = \frac{10^{19.053}}{T} e^{-134100/RT} \qquad (27)$$

A further consequence of the results listed in Figure 9 is that the third-body efficiency of atomic F for the recombination of H and F atoms is not grossly different from the efficiency of Ar atoms. For

shots 49 through 53, the atomic F content of the reacting gas immediately behind the shock wave is 11%, yet no significant effect is noted in the values of k_1, except possibly at low temperature (ca. 4100°K).

C. Rate Constants from Computer Analysis

A random selection of data taken for mixes containing no added fluorine was used to evaluate the rate of the hydrogen exchange reaction, equation (11). The value of k_1 was taken from the initial slopes of these data and set equal to

$$k_1 = \frac{0.25}{T^2} \times 10^{23} \, e^{-134100/RT} \tag{28}$$

The T^{-2} dependence of the pre-exponential factor was found to give a slightly better fit for these data, Figure 9. The reaction profiles were computed for these data for each of several values of k_2 and the results were then compared with the observed profiles (see Figures 10a, 10b, and 10c). Figure 11 illustrates the effect of k_2 on the shape of the reaction profile for a single run corresponding to a mix containing added hydrogen.

The resulting best value for k_2 is given by the expression

$$k_2 = 0.2 \times 10^{13} \, e^{-35000/RT} \tag{29}$$

This value is low by a factor of five in comparison to the value obtained by Jacobs et al[1], i.e.,

$$k_2 = 0.1 \times 10^{14} \, e^{-35000/RT} \tag{30}$$

An examination of the computed profile R1 of Figure 11 with the experimental data, R4, reveals that this difference in the two values of k_2 cannot be ascribed to scatter in the experimental data.

The rates described by equations (28) and (29) were then applied to a random selection of data for mixes containing various amounts

of added fluorine. The results indicated that the value of k_1 as given

by equation (28) was slightly high at low temperatures (ca. 4000°K).

Accordingly, the values of k_1 given by (26) were tried. The results

are illustrated in Figure 12. The good fit attests to the applicability

of the selected values of k_1 and k_2.

The fact that equation (28) gives values of k_1 which are

slightly high at low temperature (ca. 15%) indicates that the value chosen

for k_2 is probably low by a small amount, as k_2 has its greatest relative

influence at low temperatures. Even though this seems probable, it does

not warrant an attempt to improve the value of k_2, as this would only

mean an increase in its value of 20% at most.

D. Recombination Rate Constants

In an effort to quantitatively reproduce the temperature de-

pendence of the rates of atom-atom recombinations, Benson and Fueno[9]

describe a cascade mechanism for vibrational deactivation of newly formed

and highly excited diatomic molecules. They assume that deactivation or

activation proceeds by collision with neighboring molecules and occurs

by one vibrational quantum at a time.

Figure 13 illustrates the agreement between our experimentally

determined recombination rates and the values given by this cascade

model. The agreement must be considered as excellent in view of the fact

that the model gives both the negative temperature dependence of the re-

combination rates as well as the correct magnitude (within a factor of

2).

Of course, the theory of Benson and Fueno[9] can be used conversely to reproduce the correct temperature dependence and magnitude of the corresponding dissociation rates of diatomic molecules. This is illustrated in Figure 9 for the cases IA and IIA of the model (see reference 9).

In all of these calculations the effective collision diameter of the collision complex was taken as just half the value given by reference 9 for homogeneous complexes. This approximation becomes necessary due to the relative inefficiency of energy transfers for collision of inert species with the heavy F end of the complex in comparison to collisions with the light H end.

E. Conclusions

In conclusion, the best fit of the experimental data is obtained for k_1 given by equation (26) and k_2 given by equation (29).

The presence of added fluorine in the reacting mix appears to have no influence on the reaction rate except for the simple mass-action suppression of reactions (10) and (11). Since the presence of added fluorine suppresses the hydrogen exchange reaction, the values of k_1 taken from the initial rates for these data should more nearly reflect reality than those values of k_1 taken from the initial rates of reaction for mixes containing no added fluorine.

The rate of reaction (13), the fluorine exchange reaction, cannot be obtained from the present study due to its apparent insignificance compared with the rates of reactions (10) and (11).

The third-body efficiency of atomic fluorine for the recombination of atomic hydrogen and fluorine does not grossly exceed the third-

23

body efficiency of argon for the same recombination.

If atomic hydrogen has an efficiency for third-body recombination of atomic hydrogen and fluorine grossly in excess of that for argon, it would be difficult to separate the effect from the effect of the hydrogen exchange reaction.

The cascade model of Benson and Fueno appears to be qualitatively and quantitatively correct when compared with the experimentally determined recombination rates of atomic H and F.

REFERENCES

1. T. A. Jacobs, R. R. Giedt, and N. Cohen, "The Kinetics of Dissociation of Hydrogen Fluoride in Shock Waves", Aerospace Corporation, Report No. TDR-469 (5240-20)-10, 1965.

2. J. F. Spinnler, "Shock Tube Studies of the Dissociation Rate of Hydrogen Fluoride", Quarterly Progress Report in Interior Ballistics, No. P-64-22, Defense Documentation Center No. AD 355643, Rohm and Haas Company, Huntsville, Alabama, November 1964. CONFIDENTIAL

3. Raymond L. Oglukian, "Determination of the Dissociation Rate of Fluorine", Technical Report No. AFRPL-TR-65-152, October 1965.

4. S. S. Penner, "Quantitative Molecular Spectroscopy and Gas Emissivities", pp. 28-31, Addison-Wesley Publishing Company, Inc., Reading, Mass (1959).

5. B. Oksengorn, Spectrochimica Acta 19, 541 (1943).

6. W. Malkmus, "Infrared Emissivities of Diatomic Gases with Doppler Line Shape", General Dynamics/Convair, Report No. ZPh - 119 (1961).

7. G. A. Kuiper, J. Mol. Spectroscopy, 2, 75 (1958).

8. JANAF Thermochemical Tables, Dow Chemical Co., Midland, Michigan, July 1966.

9. Sidney W. Benson and Takayuki Fueno, J. Chem. Phys, 36, 1597 (1962).

TABLE I

INTERNAL CONSISTENCY OF INITIAL EMISSION INTENSITIES

First Set*

Run No.	$T^\circ K$	$C^\circ_{HF} \times 10^6$ (moles/cc)	E° (Volts)	$(E^\circ/C^\circ_{HF} \times 10^{-6})$
49	4175	0.238	1.04	4.4
53	4264	0.285	1.54	5.4
50	4312	0.185	0.95	5.1
54	4426	0.426	2.23	5.2
51	4784	0.176	0.89	5.1
52	5283	0.112	0.59	5.3
47	5613	0.200	0.87	4.4

Second Set

Run No.	$T^\circ K$	$C^\circ_{HF} \times 10^6$ (moles/cc)	E° (Volts)	$(E^\circ/C^\circ_{HF} \times 10^{-6})$
71	3231	0.086	0.82	9.5
69	3932	0.081	0.71	8.8
70	3961	0.102	0.92	9.0
72	4260	0.185	1.37	7.4
66	6105	0.098	0.68	7.0
67	6276	0.077	0.82	10.6
68	6365	0.077	0.76	9.9

*Refers to individual settings for bias current and amplifier plate voltage.

TABLE II

COMPOSITIONS AND SHOCK PARAMETERS FOR INDIVIDUAL SHOTS

Shot No.	% HF	% H_2	% F_2	U^* (mm/μsec)	εU^{**} (mm/μsec)	$T_i°K^†$	$T_f°K^†$	$C^\circ_{HF} \times 10^7$ (mole/cc)	$k_1 \times 10^{-11}$ (cc/mole sec)
40	2.17	0.00	0.00	2.455	0.035	5563	5053	1.44	0.0282
41	2.12	0.00	0.00	2.410	0.030	5370	4872	1.43	0.000539
42	2.12	0.00	0.00	2.410	0.019	5379	4881	1.43	0.0337
43	2.12	0.00	0.00	2.363	0.025	5174	4676	1.43	0.0201
44	3.03	0.00	0.00	2.324	0.034	4970	4386	2.55	0.00953
45	2.95	0.00	0.00	2.019	0.022	3822	3613	2.43	0.000574
46	2.95	0.00	0.00	1.983	0.015	3696	3525	2.43	0.000233
47	2.95	0.00	0.00	2.477	0.038	5613	4917	2.00	0.0278
48	Velocity Trace Failed			—	—	—			—
49	2.52	0.00	5.84	2.270	0.023	4138	4053	2.38	0.000539
50	2.45	0.00	5.84	2.272	0.028	4145	4046	1.85	0.00109
51	3.12	0.00	5.34	2.437	0.024	4784	4410	1.76	0.00430
52	3.02	0.00	5.84	2.469	0.035	4914	4414	1.17	0.0105
53	3.02	0.00	5.84	2.262	0.019	4110	4011	2.85	0.000666
54	3.75	0.00	0.00	2.191	0.015	4426	4039	4.26	0.00333
55	3.75	0.00	0.00	2.555	0.038	5905	4996	0.963	0.0679
56	2.02	5.00	0.00	2.278	0.033	4499	3794	1.74	0.0000
57	2.36	0.00	1.80	2.346	0.035	4824	4469	1.59	0.00694
58	2.35	0.00	1.80	2.358	0.025	4871	4473	0.949	0.0161
59	2.52	0.00	1.80	2.551	0.028	5672	5161	1.71	0.0244
60	2.47	0.00	1.80	2.595	0.037	5862	5350	1.01	0.0635
61	3.57	0.00	0.00	2.641	0.024	6314	5479	1.37	0.0693
62	1.34	0.00	0.922	2.589	0.033	6022	5739	0.570	0.0822
63	1.39	0.00	0.922	2.656	0.048	6320	6054	0.559	0.127
64	1.39	0.00	0.922	2.150	0.009	4218	4041	0.546	0.00305
65	1.92	0.00	0.375	2.474	0.025	5613	5146	0.766	0.0371
66	1.92	0.00	0.375	2.583	0.044	6102	5623	0.977	0.0741
67	1.92	0.00	0.375	2.624	0.030	6276	5808	0.770	0.140
68	1.92	0.00	0.375	2.646	0.037	6365	5909	0.771	0.116
69	2.07	0.00	0.375	2.050	0.027	3932	3711	0.807	0.0000

TABLE II (CONTINUED)

Shot No.	% HF	% H_2	% F_2	U^* (mm/μsec)	SU^{**} (mm/μsec)	T_i °K[†]	T_f °K[‡]	C^o_{HF} x 10^7 (mole/cc)	k_1 x 10^{-11} (cc/mole sec)
70	2.06	0.00	0.375	2.058	0.020	3961	3747	1.02	0.0000
71	2.06	0.00	0.375	1.849	0.023	3231	3203	0.790	0.0000
72	2.06	0.00	0.375	2.140	--	4260	3992	1.71	0.0000
73	0.984	0.00	0.00	2.161	0.023	4425	4166	0.808	0.00320
74	0.984	0.00	0.00	1.871	0.020	3379	3323	0.792	0.0000
75	0.984	0.00	0.00	1.775	0.020	3068	3043	0.784	0.0000
76	1.03	0.00	0.00	2.250	0.026	4768	4528	0.631	0.00784
77	1.02	0.00	0.00	2.339	0.071	5150	4851	0.508	0.0213
78	1.02	0.00	0.00	2.359	0.046	5216	4966	0.400	0.0278
79	2.05	0.00	2.97	2.171	0.016	4089	3989	1.75	0.000614
80	2.05	0.00	2.97	2.330	0.028	4700	4385	1.06	0.00355
81	2.05	0.00	2.97	2.285	0.014	4522	4426	1.06	0.00256
82	2.05	0.00	2.97	Velocity Trace Failure					
83	2.05	0.00	2.97	2.042	0.014	3621	3603	1.04	0.0000
84	Defective Oscillogram					--	--	--	--
85	1.93	0.00	2.97	2.554	0.032	5635	5209	1.00	0.0266
86	1.95	0.00	2.97	2.526	0.023	5513	5089	1.01	0.0256
87	1.95	0.00	2.97	2.442	0.021	5155	4768	1.01	0.0229
88	1.95	0.00	2.97	2.663	0.021	6109	5669	0.510	0.104
89	0.852	0.00	0.00	2.382	0.036	5320	5096	0.452	0.0341
90	0.911	0.00	0.00	2.489	0.024	5784	5558	0.455	0.0469
91	1.96	0.323	0.00	2.553	0.029	5977	5432	0.992	0.0930
92	1.97	0.323	0.00	2.418	0.022	5390	4859	0.991	0.0333
93	1.97	0.323	0.00	1.716	0.017	2849	2816	0.940	0.0000
94	1.97	0.323	0.00	2.374	0.021	5206	4687	0.989	0.0185
95	1.97	0.323	0.00	2.592	0.014	6153	5602	0.998	0.0775
96	0.00	0.00	0.00	2.366	0.049	5300	5300	0.000	--
97	0.00	0.323	0.00	2.354	0.019	5124	4614	0.983	0.0183
98	1.97	0.323	0.00	2.138	0.015	4274	3931	0.976	0.00149
99	2.23	0.00	1.48	2.452	0.028	5367	4893	1.47	0.0166
100	2.16	0.00	1.48	2.463	0.026	5413	4938	1.46	0.0146
101	2.16	0.00	1.48	2.543	0.011	5756	5253	0.736	0.0466

*Shock Velocity
**Standard Deviation of Shock Velocity

† Temperature of Gas Immediately Behind Shock Wave.
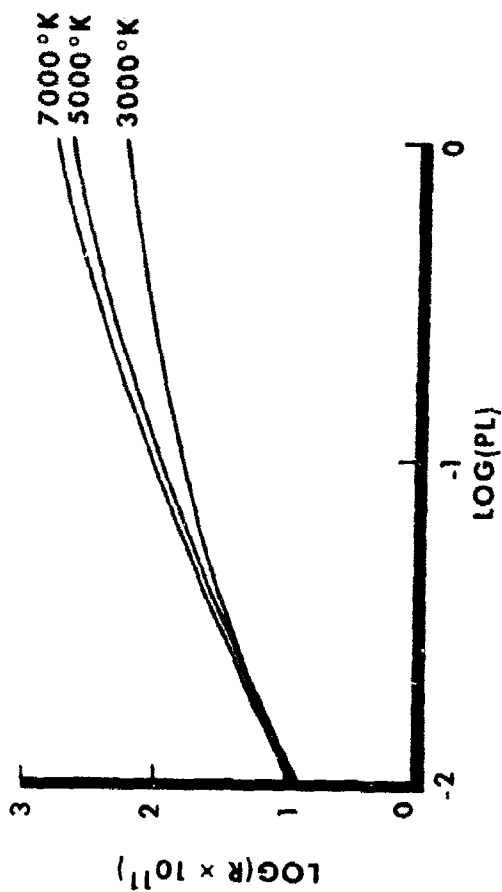‡ Temperature of Gas at Equilibrium.

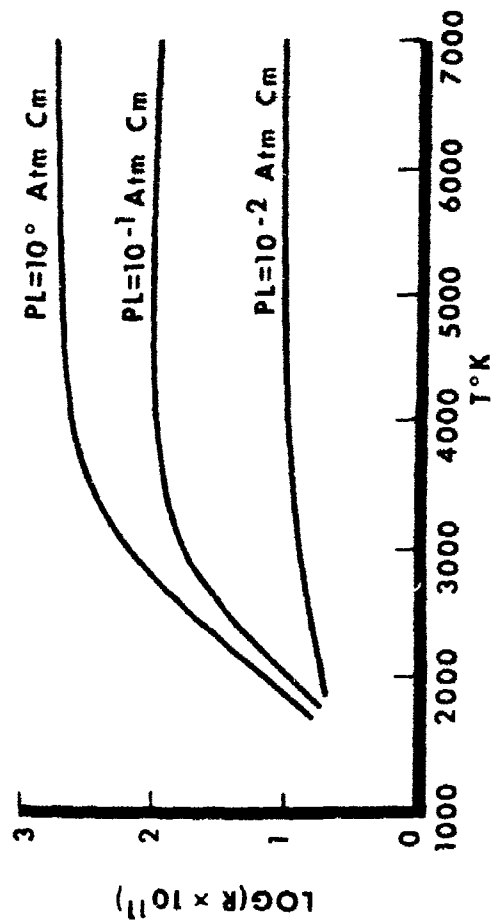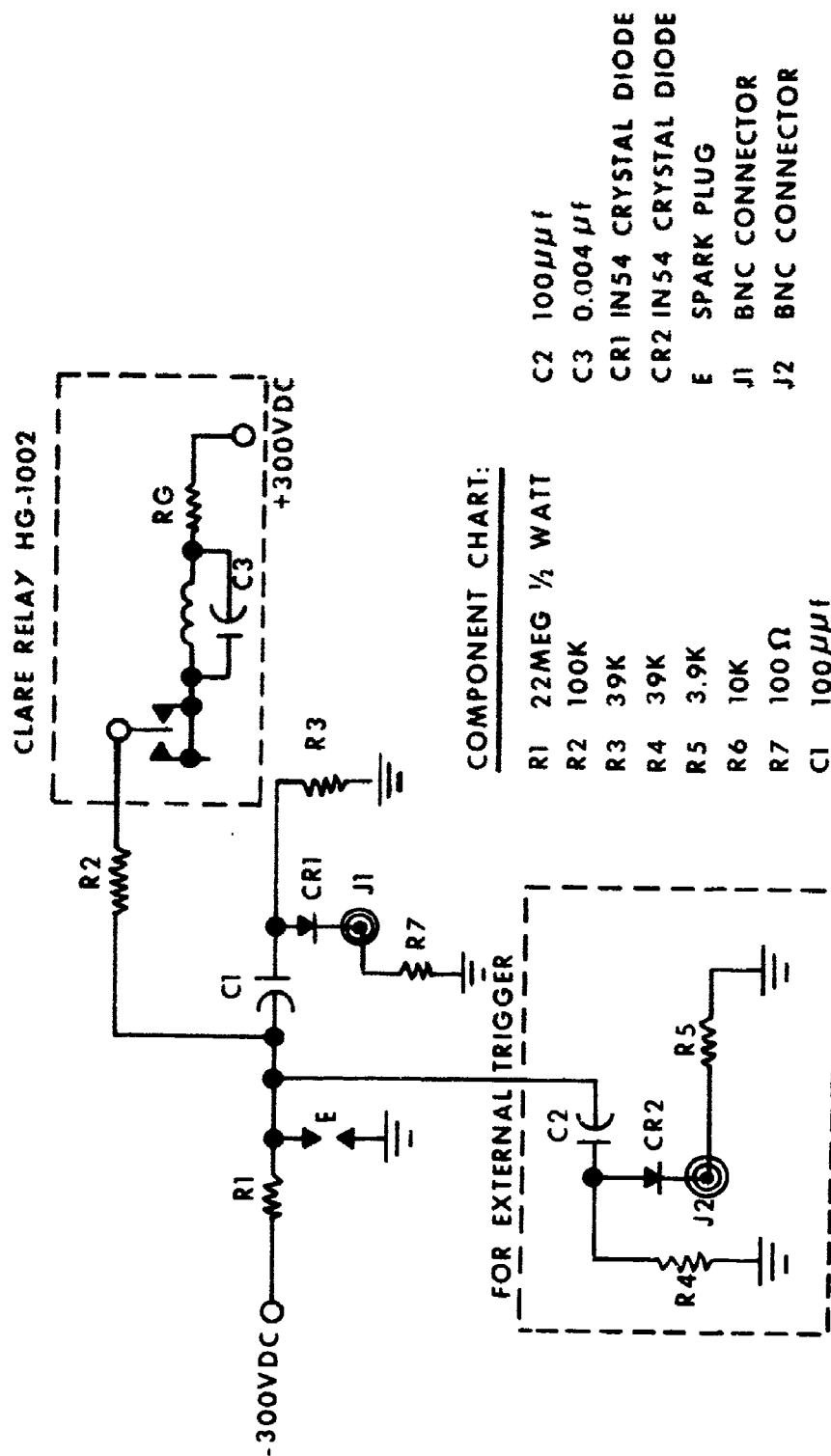**Fig. 1, SPECTRAL RADIANCY AS A FUNCTION OF OPTICAL DENSITY**

Fig. 2, SPECTRAL RADIANCY AS A FUNCTION OF TEMPERATURE

CLARE RELAY HG-1002

RG

C3

+300VDC

R2

R3

CR1 J1

R7

C1

E

R1

-300VDC

FOR EXTERNAL TRIGGER

C2

CR2

R5

J2

R4

COMPONENT CHART:

R1 22MEG ½ WATT
R2 100K
R3 39K
R4 39K
R5 3.9K
R6 10K
R7 100 Ω
C1 100 μμf

C2 100 μμf
C3 0.004 μf
CR1 IN54 CRYSTAL DIODE
CR2 IN54 CRYSTAL DIODE
E SPARK PLUG
J1 BNC CONNECTOR
J2 BNC CONNECTOR

Fig. 3, SCHEMATIC DIAGRAM OF SPARK SIGNAL BOX
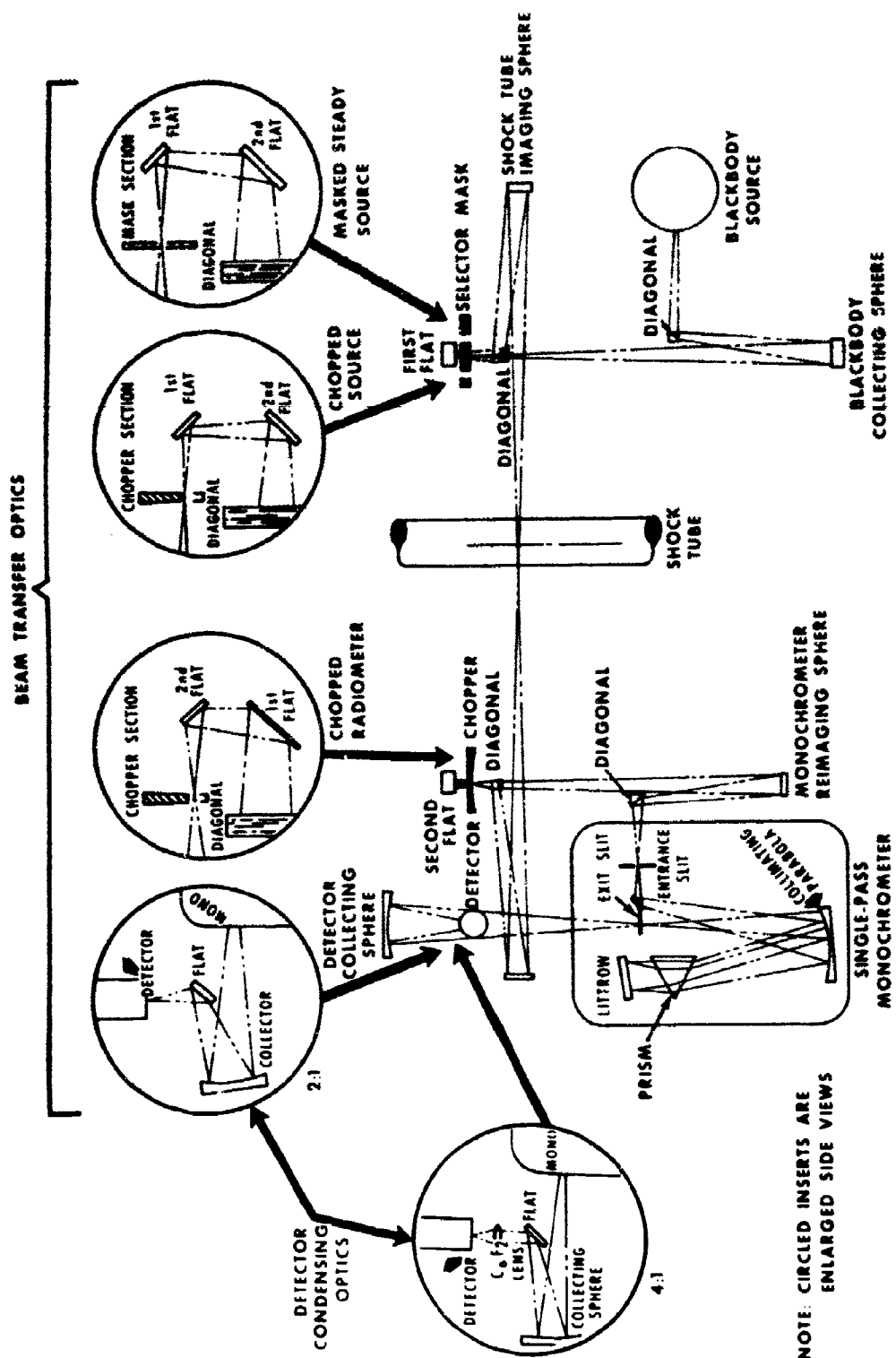(ONE FOR EACH SPARK PLUG)
AS PER AVCO RESEARCH CO.

30

Fig. 4, SCHEMATIC OF THE INFRARED SPECTROPHOTOMETER OPTICS

NOTE: CIRCLED INSERTS ARE
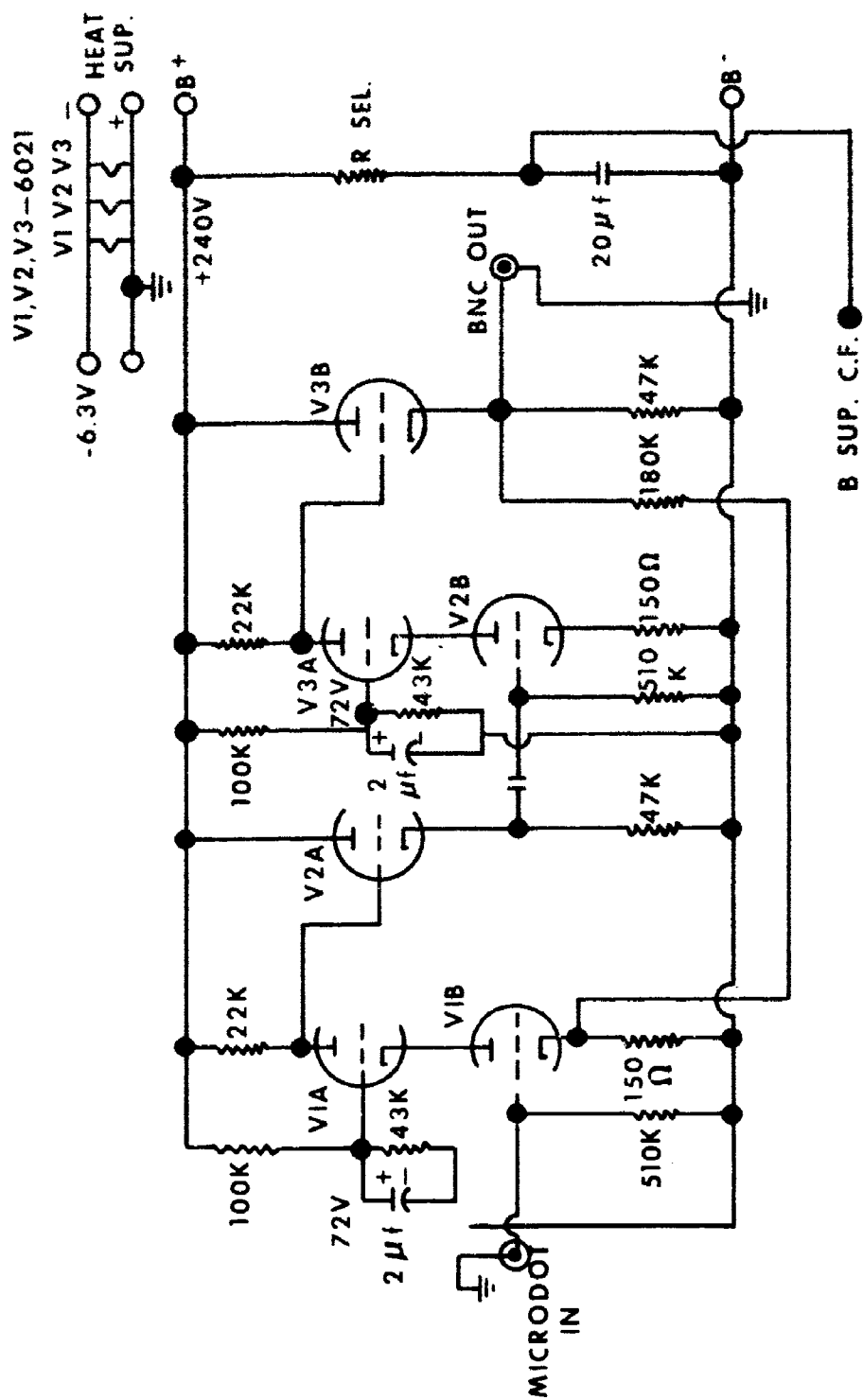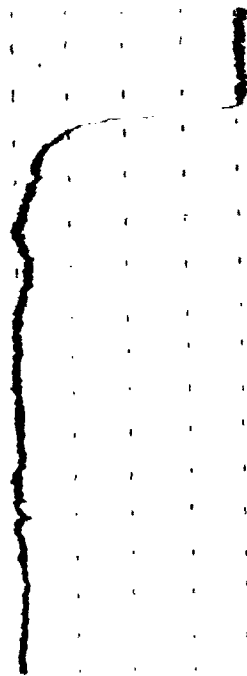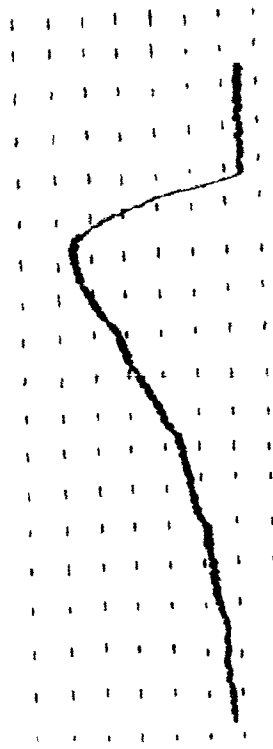ENLARGED SIDE VIEWS

31

Fig. 5, SCHEMATIC OF DETECTOR BIAS SUPPLY

Fig. 6, SCHEMATIC OF DETECTOR AMPLIFIER

33

Fig.7b, REACTION PROFILE FOR
SHOT NO.99 2.23%HF, 1.48%F$_2$,
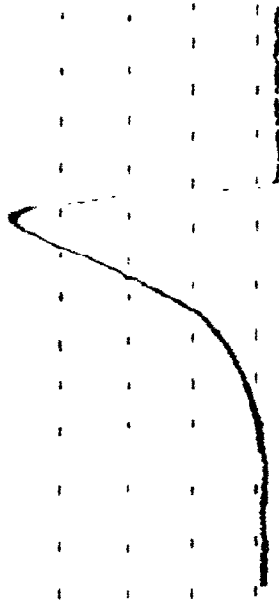5367°K, 5μ SEC TIME MARKS
0.1 VOLT ORDINATE DIVISIONS

Fig.7a, REACTION PROFILE FOR
SHOT NO.71 2.06%HF,0.375%F$_2$,
3231°K,10μ SEC TIME MARKERS,
0.2 VOLT ORDINATE DIVISIONS

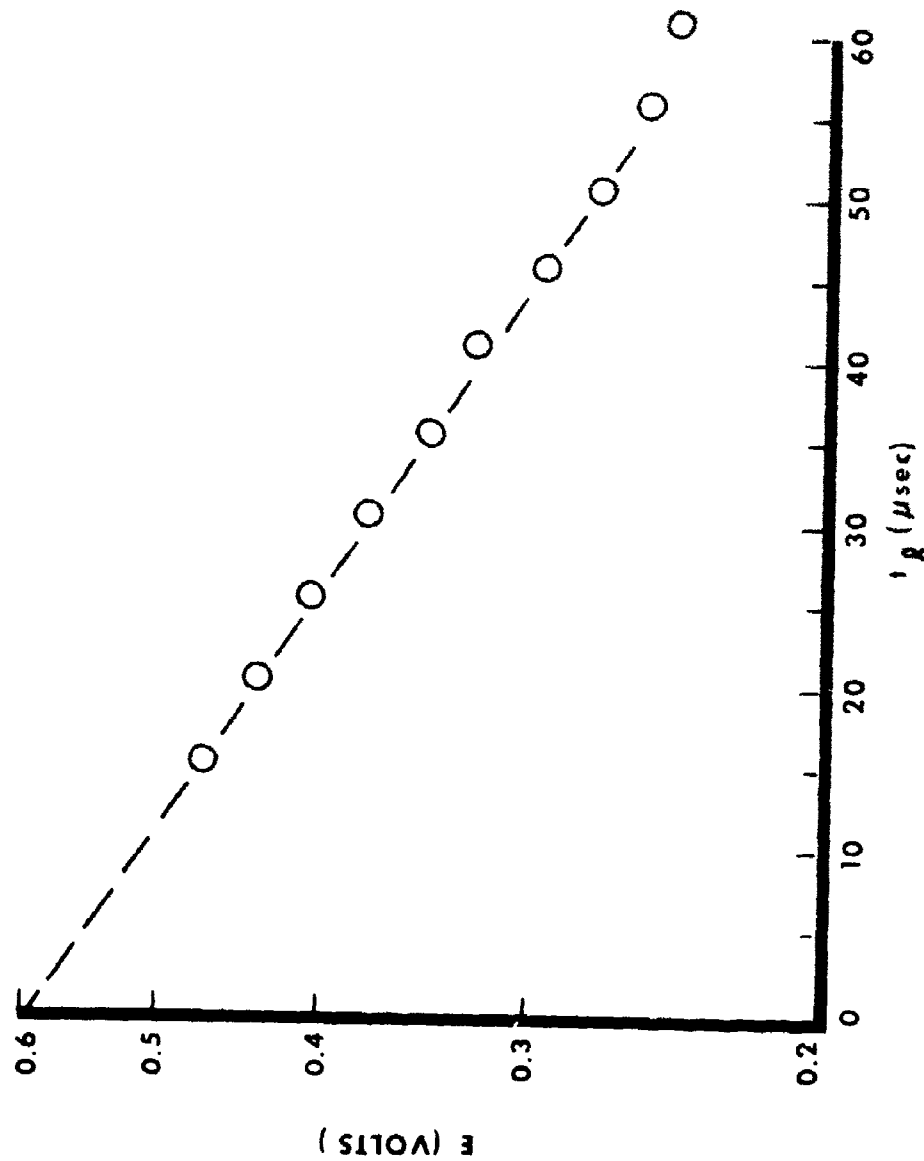Fig.7d, REACTION PROFILE FOR
SHOT NO.60 2.47%HF, 1.80%F_2,
5862°K, 10μ SEC TIME MARKS
0.1 VOLT ORDINATE DIVISIONS

Fig. 7c, REACTION PROFILE FOR
SHOT NO.58 2.35%HF, 1.80%F_2,
10μSEC. TIME MARKS 0.2 VOLT,
ORDINATE DIVISIONS,4871°K

35

Fig. 8, LOGARITHMIC EXTRAPOLATION ILLUSTRATED FOR SHOT NO. 52, 5.84% F_2, 3.02% HF, 5283°K

36

Legend:
△ — 0%F_2, 0%H_2
▲ — 0.323%H_2
□ — 0.375%F_2
⊠ — 1.48%F_2
● — 1.80%F_2
⊕ — 2.97%F_2
◓ — 5.84%F_2

$$k_1 = \frac{0.47 \times 10^{19}}{T} e^{-134100/RT}$$

$$k_1 = \frac{0.22 \times 10^{23}}{T^2} e^{-134100/RT}$$

∞∞∞∞ BENSON & FUENO 1A
ooooo BENSON & FUENO 11A

k_1(LITERS/MOLE SEC)

$(1/T)°K^{-1}$
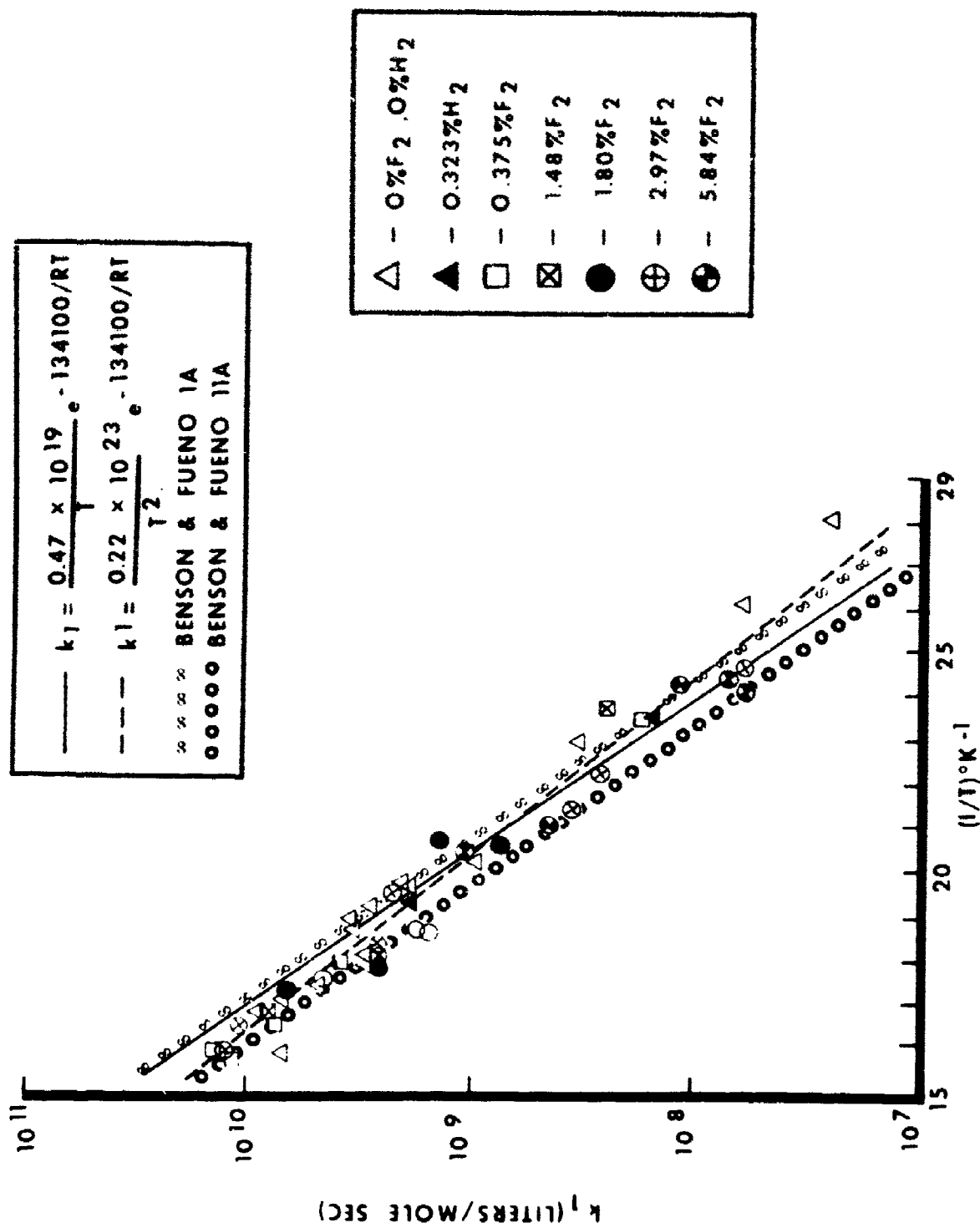
Fig. 9, TEMPERATURE DEPENDENCE OF INITIAL RATES

Fig. 10g. COMPARISON OF COMPUTED & OBSERVED REACTION PROFILES FOR MIXES CONTAINING NO ADDED FLUORINE; k_2 TOO LARGE

The figure contains the following legend table:

SYMBOL	RUN	T(initial)	T(final)	%H$_2$
A	45	3821	3614	0.0
B	98	4274	3931	0.32
C	76	4769	4528	0.0
D	94	5206	4687	0.32

Rate equations shown on plot:

$$k_1 = \frac{0.25}{T^2} \times 10^{23} \exp\left(-\frac{134100}{RT}\right)$$

$$k_2 = 0.4 \times 10^{13} \exp\left(-\frac{35000}{RT}\right)$$

$$k'_2 = 2k_2$$

Axis labels: vertical axis (HF)/(HF); horizontal axis LABORATORY TIME (μSEC)
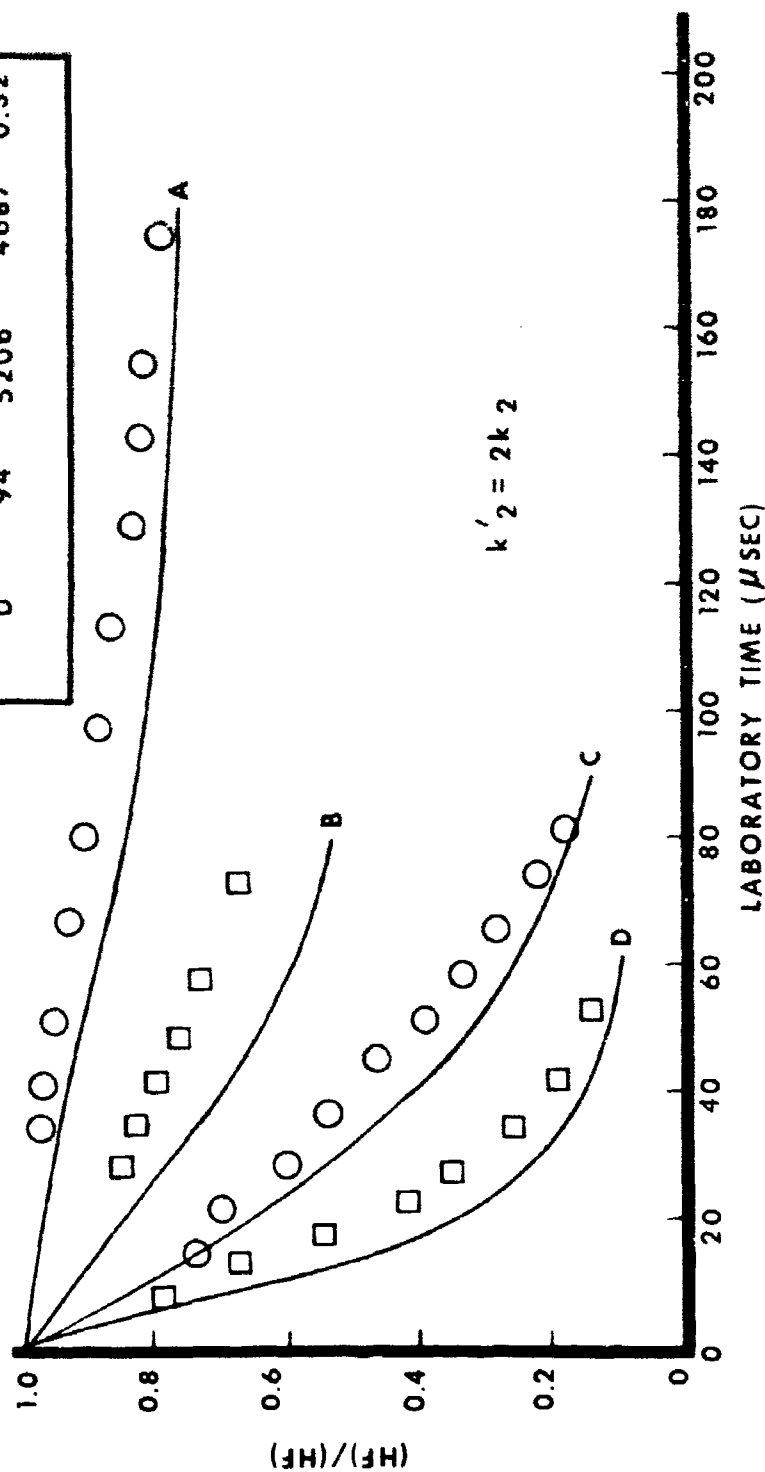
SYMBOL RUN	T(initial)	T(final)	%H_2
A 45	3821	3614	0.0
B 98	4274	3931	0.32
C 76	4769	4528	0.0
D 94	5206	4687	0.32

$$k_1 = \frac{0.25 \times 10^{23}}{T^2} \exp\left(-\frac{134100}{RT}\right)$$

$$k'_2 = 0.10 \times 10^{13} \exp\left(-\frac{35000}{RT}\right)$$

$$k'_2 = \tfrac{1}{2} k_2$$

LABORATORY TIME (μ sec)

$(HF)/(HF)_\circ$
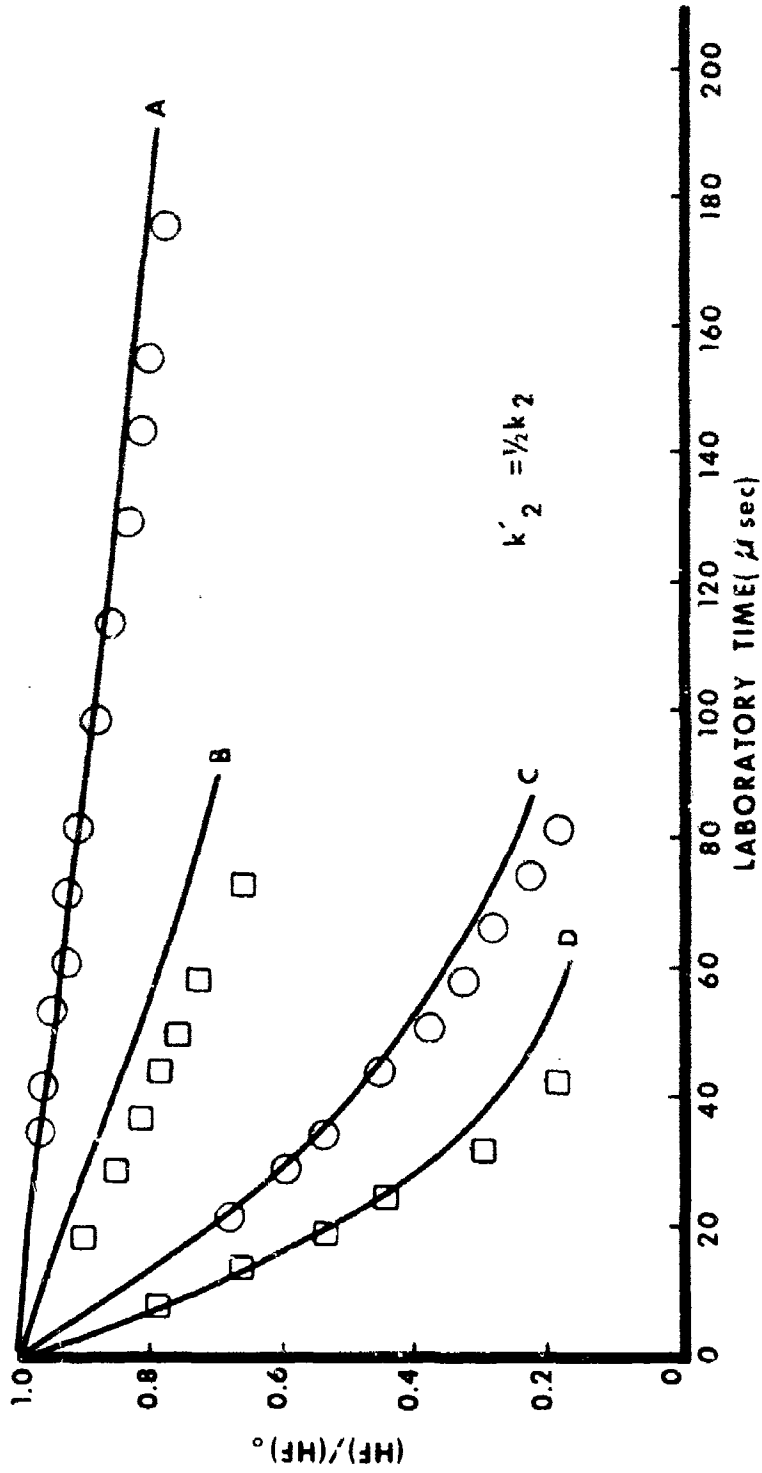
Fig. 10b, COMPARISON OF COMPUTED & OBSERVED REACTION PROFILES FOR MIXES CONTAINING NO ADDED FLUORINE; k_2 TOO SMALL

39

SYMBOL	RUN	T(initial)	T(final)	%H$_2$
A	46	3697	3525	0.0
B	45	3821	3614	0.0
C	98	4274	3931	0.32
D	73	4368	4166	0.0
E	76	4769	4528	0.0
F	94	5206	4687	0.32
G	42	5379	4863	0.0
H	90	5784	5558	0.0

$$k_1 = \frac{0.25}{T^2} \times 10^{23} \exp\left(-\frac{134100}{RT}\right)$$

$$k_2 = 0.20 \times 10^{13} \exp\left(-\frac{35000}{RT}\right)$$
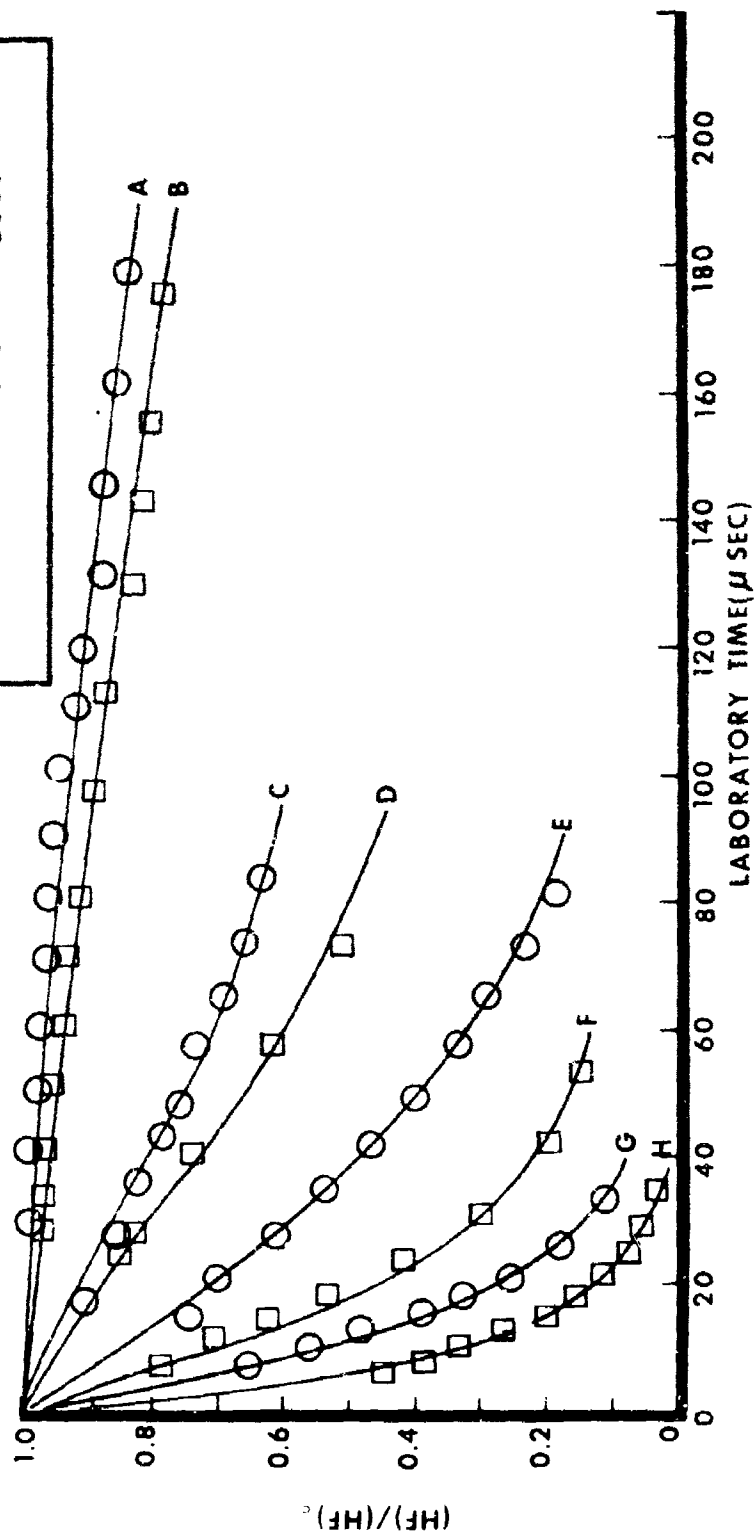
LABORATORY TIME(μ SEC)

$(HF)/(HF)_c$

Fig. 10c., COMPARISON OF COMPUTED & OBSERVED REACTION PROFILES FOR MIXES CONTAINING NO ADDED FLUORINE; BEST VALUE FOR k$_2$

40

$R1 \quad ---- \quad k_2 = 0.10 \times 10^{14} \ \exp\left(-\dfrac{35000}{RT}\right)$

$R2 \quad ---- \quad k_2 = 0.04 \times 10^{14} \ \exp\left(-\dfrac{35000}{RT}\right)$

$R3 \quad ---- \quad k_2 = 0.01 \times 10^{14} \ \exp\left(-\dfrac{35000}{RT}\right)$

$R4 \quad ---- \quad k_2 = 0.02 \times 10^{14} \ \exp\left(-\dfrac{35000}{RT}\right)$

$k_1 = \dfrac{0.25 \times 10^{23}}{T^2} \ \exp\left(-\dfrac{134100}{RT}\right)$
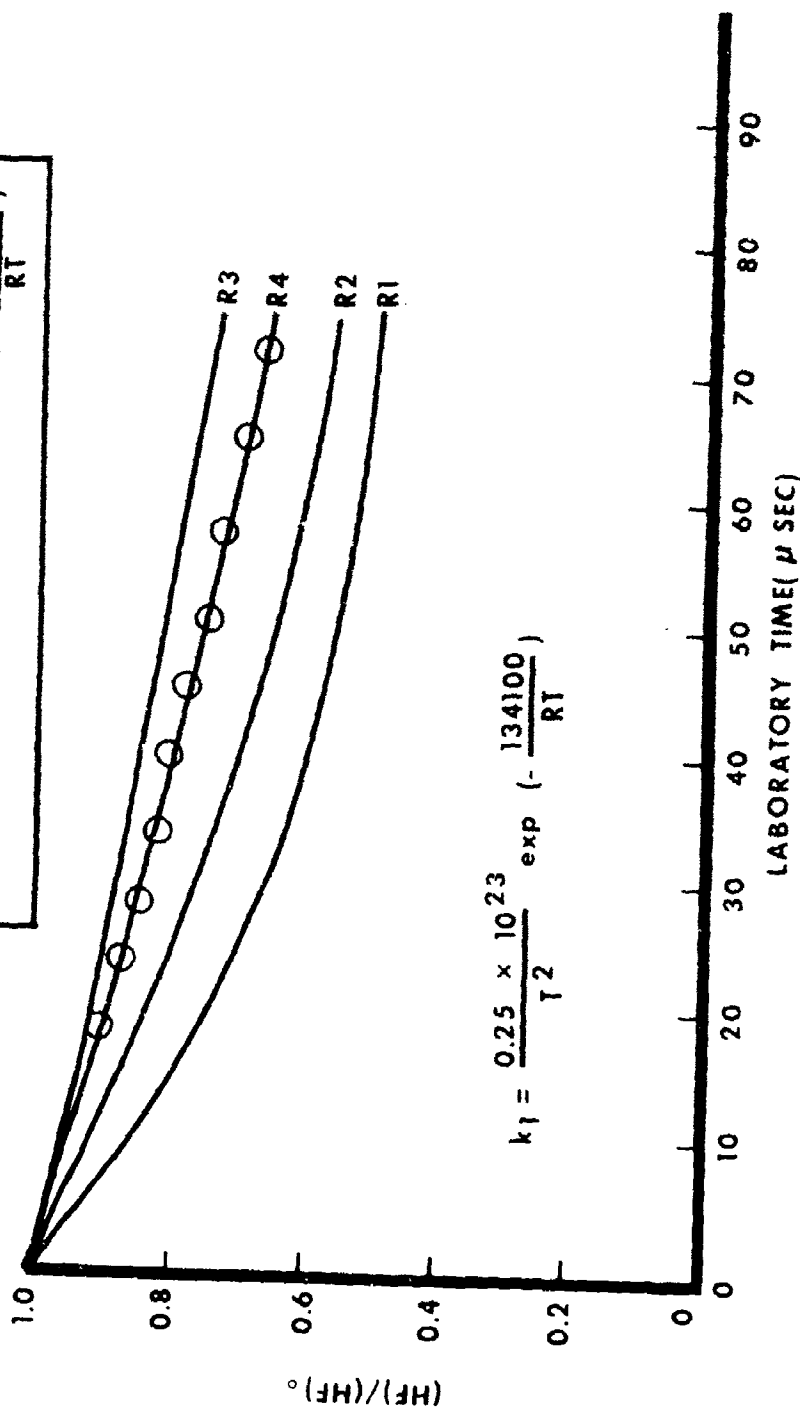
(HF)/(HF)$_0$

LABORATORY TIME (μ SEC)

R3
R4
R2
R1

Fig. 11, ILLUSTRATION OF THE DEPENDENCE OF THE REACTION PROFILE ON THE VALUE OF k_2 1.97% HF, 0.32% H_2 , 4274°K INITIALLY, SHOT NO. 98

41

SYMBOL	RUN	T(initial)	T(final)	%F$_2$
A	53	4110	3979	5.84
B	70	3961	3747	0.38
C	72	4260	3992	0.38
D	51	4785	4410	5.84
E	57	4824	4469	1.80
F	65	5613	5146	0.38
G	60	5862	5350	1.80

$$k_1 = \frac{0.47 \times 10^{19}}{T} \exp\left(-\frac{134100}{RT}\right)$$

$$k_2 = 0.20 \times 10^{13} \exp\left(-\frac{35000}{RT}\right)$$

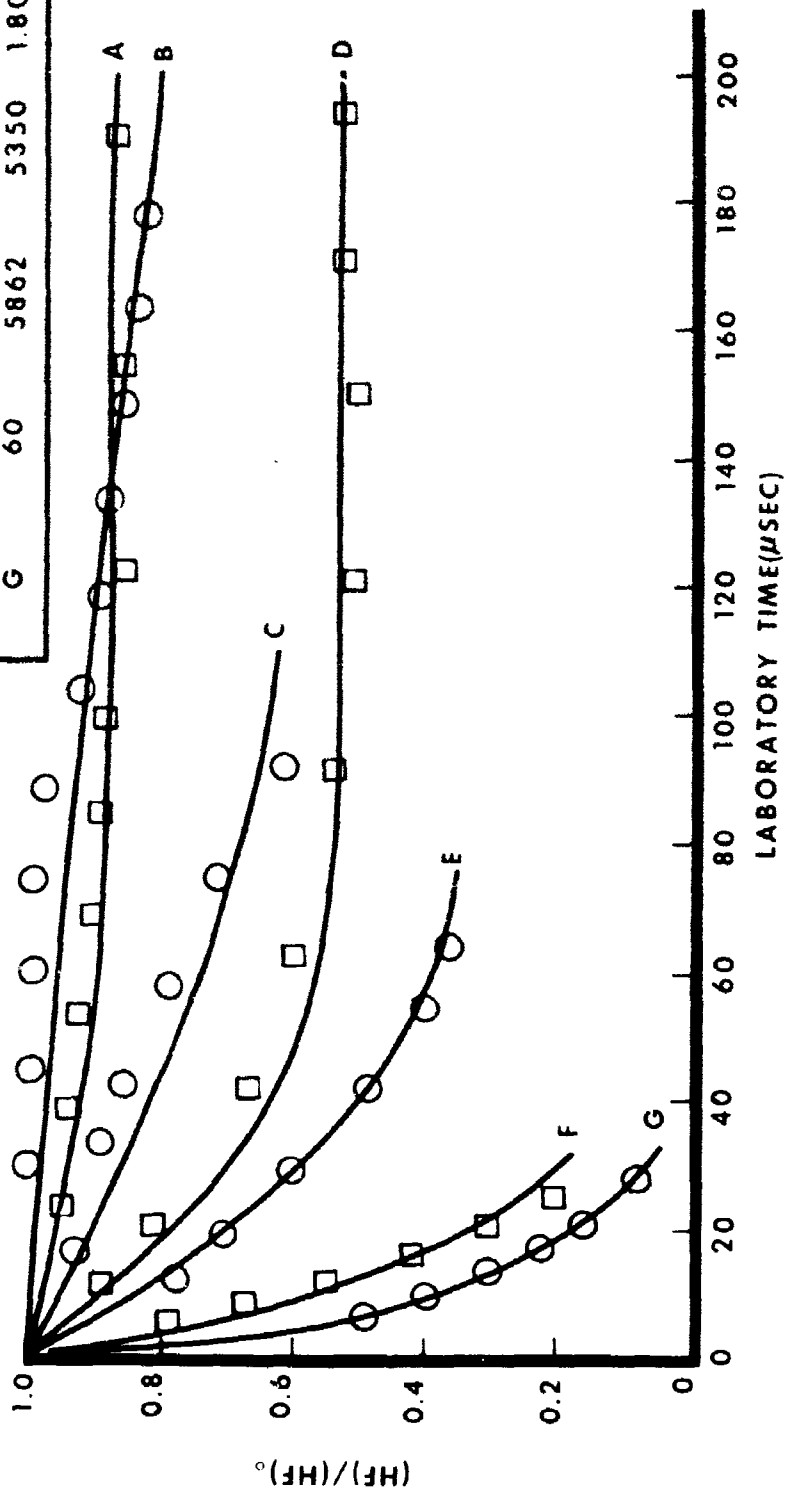LABORATORY TIME(μSEC)

(HF)/(HF)$_0$

Fig.12, COMPARISON OF COMPUTED & OBSERVED REACTION PROFILES FOR MIXES CONTAINING ADDED FLUORINE

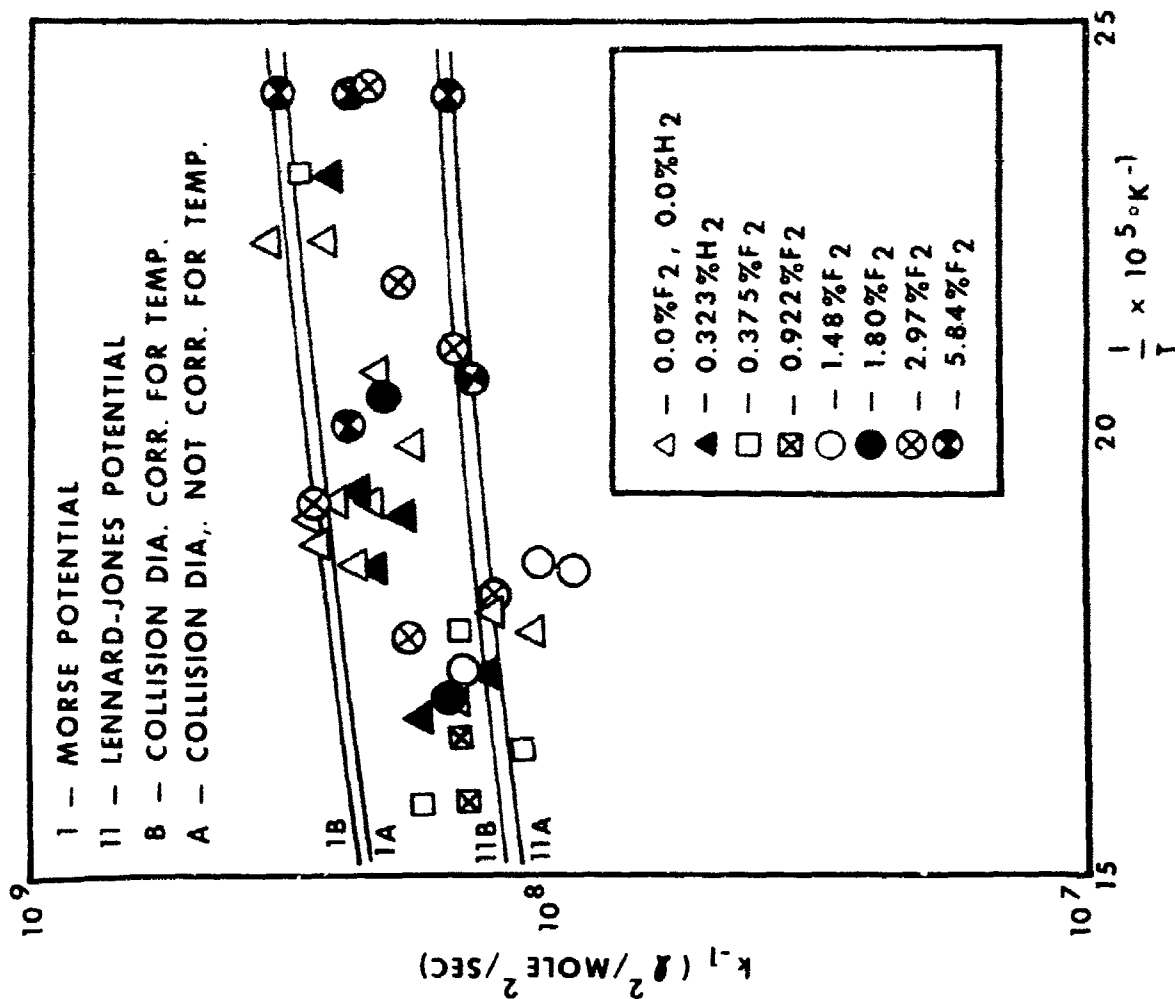Fig. 13, RECOMBINATION RATE CONSTANTS COMPARED TO THE CASCADE MODEL OF BENSON & FUENO (Ref.9)

43

DOCUMENT CONTROL DATA - R&D

(Security classification of title, body of abstract and indexing annotation must be entered when the overall report is classified)

1. ORIGINATING ACTIVITY (Corporate author)	2a. REPORT SECURITY CLASSIFICATION
Air Force Rocket Propulsion Laboratory Edwards, California 93523	Unclassified
	2b. GROUP N/A

3 REPORT TITLE

The dissociation Rate of Hydrogen Fluoride Behind Incident Shock Waves.

4. DESCRIPTIVE NOTES (Type of report and inclusive dates)

Phase Report, Shock Tube Kinetic Studies, January 1965 - December 1966

5. AUTHOR(S) (Last name, first name, initial)

Blauer, Dr. Jay A.

6. REPORT DATE	7a. TOTAL NO. OF PAGES	7b. NO. OF REFS
March 1967		9

8a. CONTRACT OR GRANT NO.	9a. ORIGINATOR'S REPORT NUMBER(S)
b. PROJECT NO. 3148	AFRPL-TR-67-66
c.	9b. OTHER REPORT NO(S) (Any other numbers that may be assigned this report)
d.	

10. AVAILABILITY/LIMITATION NOTICES

Distribution of this document is unlimited.

11. SUPPLEMENTARY NOTES	12. SPONSORING MILITARY ACTIVITY See Block 1

13. ABSTRACT   The rate of dissociation of hydrogen fluoride behind incident shock waves has been studied in the temperature range of 3700 to 6100°K. Gaseous mixtures containing 0 to 4% hydrogen fluoride, 0 to 6% molecular fluorine, and 0 to 0.5% molecular hydrogen in an argon carrier were used in this study. The course of the dissociation was followed by monitoring the emission intensity of the 1-0 band of hydrogen fluoride at 2.5μ.

Resort was made to a determination of initial reaction rates to obtain values for the rate constant of the reaction $HF + M = H + F + M$. The expression $k_1 = \frac{0.47 \times 10^{19}}{T} e^{-134100/RT}$ was found to give the best fit to all of the data. The effect of excess fluorine upon the initial reaction rate demonstrated that the reaction $F + HF = F_2 + H$ is inconsequential to the present study. Similarly, it was found that atomic fluorine has roughly the same third-body efficiency as argon for the recombination of H and F.

Computer calculations based upon the whole reaction profile and including all the data indicate a value for the rate of the hydrogen exchange reaction, namely, $HF + H = H_2 + F$, of $k_2 = 2 \times 10^{12} e^{-35000/RT}$.

The data were too scattered to allow an accurate determination of the temperature dependencies of the pre-exponential factors.

DD FORM 1473
JAN 64

KEY WORDS	LINK A		LINK B		LINK C	
	ROLE	WT	ROLE	WT	ROLE	WT
Hydrogen Fluoride Dissociation						
Infrared emission measurements						
2500° K temperature range						

INSTRUCTIONS

1. ORIGINATING ACTIVITY: Enter the name and address of the contractor, subcontractor, grantee, Department of Defense activity or other organization (corporate author) issuing the report.

2a. REPORT SECURITY CLASSIFICATION: Enter the overall security classification of the report. Indicate whether "Restricted Data" is included. Marking is to be in accordance with appropriate security regulations.

2b. GROUP: Automatic downgrading is specified in DoD Directive 5200.10 and Armed Forces Industrial Manual. Enter the group number. Also, when applicable, show that optional markings have been used for Group 3 and Group 4 as authorized.

3. REPORT TITLE: Enter the complete report title in all capital letters. Titles in all cases should be unclassified. If a meaningful title cannot be selected without classification, show title classification in all capitals in parenthesis immediately following the title.

4. DESCRIPTIVE NOTES: If appropriate, enter the type of report, e.g., interim, progress, summary, annual, or final. Give the inclusive dates when a specific reporting period is covered.

5. AUTHOR(S): Enter the name(s) of author(s) as shown on or in the report. Enter last name, first name, middle initial. If military, show rank and branch of service. The name of the principal author is an absolute minimum requirement.

6. REPORT DATE: Enter the date of the report as day, month, year; or month, year. If more than one date appears on the report, use date of publication.

7a. TOTAL NUMBER OF PAGES: The total page count should follow normal pagination procedures, i.e., enter the number of pages containing information.

7b. NUMBER OF REFERENCES: Enter the total number of references cited in the report.

8a. CONTRACT OR GRANT NUMBER: If appropriate, enter the applicable number of the contract or grant under which the report was written.

8b, 8c, & 8d. PROJECT NUMBER: Enter the appropriate military department identification, such as project number, subproject number, system numbers, task number, etc.

9a. ORIGINATOR'S REPORT NUMBER(S): Enter the official report number by which the document will be identified and controlled by the originating activity. This number must be unique to this report.

9b. OTHER REPORT NUMBER(S): If the report has been assigned any other report numbers (either by the originator or by the sponsor), also enter this number(s).

10. AVAILABILITY/LIMITATION NOTICES: Enter any limitations on further dissemination of the report, other than those imposed by security classification, using standard statements such as:

(1) "Qualified requesters may obtain copies of this report from DDC."

(2) "Foreign announcement and dissemination of this report by DDC is not authorized."

(3) "U. S. Government agencies may obtain copies of this report directly from DDC. Other qualified DDC users shall request through

_____ ."

(4) "U. S. military agencies may obtain copies of this report directly from DDC. Other qualified users shall request through

_____ ."

(5) "All distribution of this report is controlled. Qualified DDC users shall request through

_____ ."

If the report has been furnished to the Office of Technical Services, Department of Commerce, for sale to the public, indicate this fact and enter the price, if known.

11. SUPPLEMENTARY NOTES: Use for additional explanatory notes.

12. SPONSORING MILITARY ACTIVITY: Enter the name of the departmental project office or laboratory sponsoring (paying for) the research and development. Include address.

13. ABSTRACT: Enter an abstract giving a brief and factual summary of the document indicative of the report, even though it may also appear elsewhere in the body of the technical report. If additional space is required, a continuation sheet shall be attached.

It is highly desirable that the abstract of classified reports be unclassified. Each paragraph of the abstract shall end with an indication of the military security classification of the information in the paragraph, represented as (TS), (S), (C), or (U).

There is no limitation on the length of the abstract. However, the suggested length is from 150 to 225 words.

14. KEY WORDS: Key words are technically meaningful terms or short phrases that characterize a report and may be used as index entries for cataloging the report. Key words must be selected so that no security classification is required. Identifiers, such as equipment model designation, trade name, military project code name, geographic location, may be used as key words but will be followed by an indication of technical context. The assignment of links, rules, and weights is optional.